Applied Catalysis A: General 452 (2013) 88–93

Contents lists available at SciVerse ScienceDirect

Applied Catalysis A: General

journal homepage: www.elsevier.com/locate/apcata

Effect of structure of $CuO/ZnO/Al_2O_3$ composites on catalytic performance for hydrogenation of fatty acid ester

Limin He[a,b,c], Haiyang Cheng[a,b,c], Guanfeng Liang[a,b,c], Yancun Yu[a,b], Fengyu Zhao[a,b,*]

[a] State Key Laboratory of Electroanalytical Chemistry, Changchun Institute of Applied Chemistry, Chinese Academy of Sciences, Changchun 130022, PR China
[b] Laboratory of Green Chemistry and Process, Changchun Institute of Applied Chemistry, Chinese Academy of Sciences, Changchun 130022, PR China
[c] University of the Chinese Academy of Sciences, Beijing 100049, PR China

ARTICLE INFO

Article history:
Received 5 July 2012
Received in revised form 6 November 2012
Accepted 17 November 2012
Available online 16 December 2012

Keywords:
$CuO/ZnO/Al_2O_3$
Layered double hydroxide
Hydrogenation
Fatty ester
Higher alcohol

ABSTRACT

In this work, $CuO/ZnO/Al_2O_3$ catalysts were prepared by adjusting the initial alkali concentration in the process of co-precipitation. The correlation between the structure and catalytic activity was studied, and the catalyst derived from LDHs (layered double hydroxides) structure exhibited the highest activity in the hydrogenation of fatty esters as well as high selectivity to fatty alcohol, producing fatty alcohol with a yield above 98%. The high catalytic performance was attributed to relatively high dispersion (small crystal size) and the high reducibility of copper species. In addition, the active species was discussed and the Cu^+/Cu^0 were supposed to be the active site for the present hydrogenation.

1. Introduction

The ternary composite oxide of $CuO/ZnO/Al_2O_3$ is placed on a large emphasis owing to its wide applications in steam reforming of methanol, CO hydrogenation, methanol oxidation and the water–gas shift reaction [1–5]. In recent years, the industrial catalyst of $CuO/ZnO/Al_2O_3$ has been paid more attention, and some progresses have been achieved. The most new result was reported by Behrens et al. in Science [6], they studied the active sites of the $CuO/ZnO/Al_2O_3$ catalyst in the methanol synthesis reaction by using a combination of experimental evidence and density functional theory calculations. As a result, the active site consisted of Cu steps decorated with Zn atoms, which can be stabilized by a series of well-defined bulk defects and surface species. Moreover, the investigation about the preparation methods and physicochemical properties of $Cu/ZnO/Al_2O_3$ catalyst is still desired to understand. For the preparation of $CuO/ZnO/Al_2O_3$ catalyst, several approaches have been reported, including conventional impregnation, sol–gel, precipitation, and so on [7–10], in which the co-precipitation process is not only a simple and easy method but also a promising one for fabrication of well-structured metal oxide materials with satisfied performance [11,12]. This method is simple and easy to operate; however, various factors are complex to influence the structure of precipitated intermediates, namely the precursors of the composite oxides, and finally affect the catalytic performance of the catalyst, which is an important issue and have long been investigated [13]. Remarkably, the precipitated intermediates will determine the chemical composition, particle size, surface area, pore size, pore volume of the final formed composite oxides [14–16]. Li et al. [17] reported when Al content was 12 mol%, the aurichalcite phase partially intercalated into the hydrotalcite phase, enhancing the interaction between the active centers and the support of the $Cu/ZnO/Al_2O_3$ catalyst, and finally gave a superior activity in water gas shift reaction with a CO conversion up to 97.5%. Fujita et al. [18] investigated the effect of Cu/Zn molar ratio on the components of the precursors and they found that the Cu/ZnO catalyst obtained from the precursor with aurichalcite phase (Cu/Zn = 50/50) was more active than these from malachite alone or mixed two phases for the reactions of methanol synthesis from CO_2 and the steam reforming of methanol. In addition, the pH and aging time has important influence on the structure of precursors and the final catalysts, and the results revealed that transformations and equilibrations between the preformed precursor phases and crystalline solids took place at different timescales that depend on the foregoing precipitation process [19,20]. Although numerous studies have evaluated the role of the precursor structure on the activity [20–23], few study paid attention to the structure–activity relationship and the active

* Corresponding author at: State Key Laboratory of Electroanalytical Chemistry, Changchun Institute of Applied Chemistry, Chinese Academy of Sciences, Changchun 130022, PR China. Tel.: +86 431 85262410; fax: +86 431 85262410.
E-mail address: zhaofy@ciac.jl.cn (F. Zhao).

0926-860X/$ – see front matter © 2012 Elsevier B.V. All rights reserved.
http://dx.doi.org/10.1016/j.apcata.2012.11.039

species. For example, the structure of the precipitated precursor, like the layered double hydroxides (LDHs), will impact the subsequent formation and performance of the final composite oxides [22,24,25]. Layered double hydroxides, also known as anionic clays, are a typical kind of inorganic layered mineral clays, recently, which has been extensively studied as catalysts, catalyst support, lithium battery, sensor material, electroactive and photoactive materials, ion exchangers, stabilizers, and adsorbents, etc. [26–29]. The typical LDHs compound is MgAl hydrotalcite, consequently LDHs are also known as hydrotalcites, more accurately, hydrotalcite-like materials. Owing to their special layer structures, certain acidic and basic property, these materials have attractive potential applications as catalyst or catalyst support in the future [25,29].

Herein, we focused our attention to discuss the relation of structure and catalytic performance of $CuO/ZnO/Al_2O_3$ catalysts with a model reaction of fatty ester hydrogenation. The hydrogenation of fatty ester is one of the most attractive reactions for biomass transformation in modern catalysis technology. For example, ethyl stearate could be hydrogenated to stearyl alcohol and hydrocarbons as shown in Scheme 1. The product depends on the catalyst used, the stearyl alcohol is mainly produced over the Cu based catalysts and the hydrocarbons are mainly obtained with the Ru based catalysts. For example, Cao and coworkers reported that lauryl alcohol was produced with a selectivity above 95% in the hydrogenation of methyl laurate over Cu/ZnO catalyst [23]. The fatty alcohols and their derivatives are industrially important intermediates and widely used as surfactants, lubricants, plasticizers. Industrially, fatty alcohols are mainly produced based on petrochemicals, un-renewable resources [30–32]. Natural vegetable oil is an ideal substitute for its mainly containing fatty acid with 12–20 carbon atoms and 0–3 double bonds and is cheap and inexhaustible resources from a wide variety of plants [23,33,34]. In this work, we prepared a high active $CuO/ZnO/Al_2O_3$ catalyst with the co-precipitation method by adjusting pH values with varies of the alkali concentration. The catalyst structure was studied, and we attempted to gain insight into the relationship of structure and activity of $CuO/ZnO/Al_2O_3$ catalyst for the hydrogenation of fatty acid esters to higher alcohol. Particularly, the active site was also discussed tentatively through the copper valence change combined with the experimental data.

2. Experimental

2.1. Catalyst preparation

All chemicals are analysis grades and used without further purification.

At first, an aqueous solution was prepared with copper nitrate, zinc nitrate and aluminum nitrate with molar ratio of $Cu^{2+}/Zn^{2+}/Al^{3+} = 4/2/2$, then sodium carbonate aqueous solution (0.6–2.0 M) was dropwise added into the mixture under vigorous stirring at 50 °C and the pH value was controlled and adjusted at 7.5 using a pH meter. The precipitates formed were further aged for 4 h under stirring at the same temperature, then filtrated and washed with deionized water until no sodium ion existed. The precipitated precursors were dried at 110 °C and calcined at 350 °C in air for 3 h with a heating rate of 5 °C min^{-1}, finally the formed composite oxides were collected and stored in a vessel for the later use to the hydrogenation reaction. The precursors of composites are designated as CZApre-*x*, where the "pre" is abbreviation of precursor; *x* represents the concentration of the sodium carbonate. The composite formed from the corresponding precursor calcined at 350 °C for 3 h in air is designated as CZA-*x*. In order to discuss the reaction active sites, CZA-2.0 sample was reduced under hydrogen at 230 °C for 90 min, and it was named as "pre-reduced catalyst."

Table 1
Results on the microstructure of the different catalyst precursors.

Sample	*d*-Spacing (Å) *d*(0 0 3)	Crystal size (Å)
CZApre-0.6	7.491	443
CZApre-1.0	7.452	310
CZApre-2.0	7.430	127

2.2. Catalyst characterization

The structure and crystal phase composition of the materials was determined by XRD patterns with a Brucker D8 GADDS diffractometer using Co K radiation (1.79 Å), and the crystallite size was calculated with Scherrer's equation.

The temperature-programmed reduction (TPR) analysis was performed under a flow of 5% H_2/N_2 mixture (30 ml/min), with a heating rate of 10 K/min.

Thermogravimetric analysis (TGA) was conducted on TGA/DSC 1/1100 LF (Mettler-Toledo) Thermal Analysis System in air atmosphere with a flow rate of 20 ml/min and temperature increased from room temperature to 650 °C at a heating rate of 10 K/min.

X-ray photoelectron spectroscopy (XPS, VG Microtech 3000 Multilab) was used to examine the electronic properties of the catalyst. The binding energy (BE) values were referenced to the C 1s peak of contaminant carbon at 284.6 eV with an uncertainty of ±0.2 eV.

2.3. Hydrogenation reaction

Typically, the catalytic hydrogenations were carried out in a 50 ml stainless steel autoclave. After ethyl stearate, catalyst and hexane were added, the autoclave was flushed with H_2 for three times to remove the air. Then it was pressurized with hydrogen to 3.0 MPa with a back pressure regulator. The reactions were operated under a stirring rate of 1300 rpm (without diffusion limitation). After reaction operated for several hours (as desired), the autoclave was then cooled down to room temperature, and the products were collected and analyzed by gas chromatography with FID detector with a DB-1 capillary column and GC–MS respectively.

The recycling experiments were carried out with the CZA-2.0 catalyst under the above reaction conditions. After one reaction run finished, the catalyst was separated from the reaction solution by the centrifugation and reused again directly for the next run without any treatment.

3. Results and discussion

3.1. The structure of $CuO/ZnO/Al_2O_3$ composites

The $CuO/ZnO/Al_2O_3$ composites were prepared by co-precipitation methods through adjusting the pH values with varying the Na_2CO_3 concentration as described above; the precipitate formed was named precursor CZApre-*x* and which was calcined consequently to form the final metal composite oxides CZA-*x*. The structure and phase composition of the precursor and the final composites were analyzed by XRD and TGA. From the results of XRD shown in Fig. 1, the diffraction patterns of copper or zinc nitrate hydroxide, hydrotalcite, and malachite phases were formed for CZA-0.6 and CZA-1.0 (Fig. 1A), but only hydrotalcite phase was formed for the CZA-2.0 sample. The specific parameters of the microstructure of all samples were summarized in Tables 1 and 2. Compared with CZApre-0.6 sample, the diffraction peaks of the nitrate hydroxide salts become weaker and those of malachite phase were more intensive in the CZApre-1.0 sample. The phase of copper or zinc nitrate hydroxide $(Cu, Zn)_2(OH)_3(NO_3)_3$

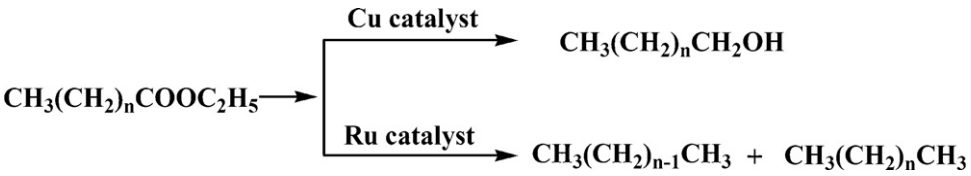

Scheme 1. Hydrogenation reaction route of aliphatic fatty ester (n = 16 for ethyl stearate).

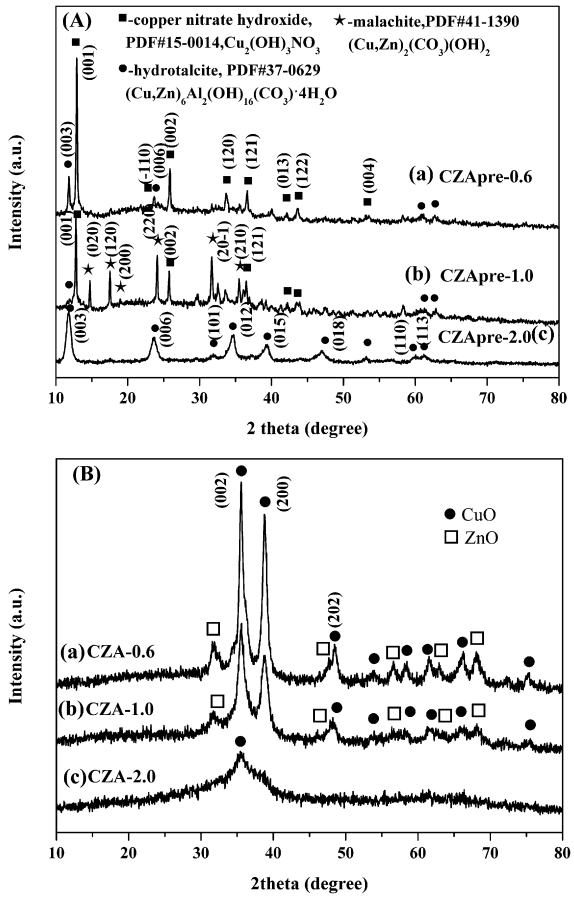

Fig. 1. The XRD patterns of catalysts precursors (A) prepared at alkali concentrate of (a) 0.6 M, (b) 1.0 M, and (c) 2.0 M; and (B) catalysts calcined at 350 °C (3 h).

was formed at the low initial alkali concentration [8,35], since the nitrate and hydroxyl metal compounds are easily to precipitate than the carbonate metal compounds due to the lower concentration of CO_3^{2-}, thus CO_3^{2-} did not present in the precursor but coordinated to form the phase of nitrate hydroxide phase. With increasing the alkali concentration to 1.0 M, the malachite phase was mainly formed and observed due to the higher saturation degree of malachite precipitate based on the precipitating rate and/or the k_{sp} of the precipitates of the metal compounds [17,36].

Table 2
Results on the characterization of calcined catalysts.

Catalyst	Crystal size (Å)[a]		T_r (°C)[b]
	CuO (0 0 2)	CuO (1 1 1)	
CZA-0.6	167	142	224, 236, 304
CZA-1.0	151	134	222, 249
CZA-2.0	124	n.d	202

[a] Calculated from the values of the full-width at half-maximum (fwhm) of the CuO (0 0 2) and CuO (1 1 1) diffraction peaks by means of the Scherrer' equation.
[b] Tr represents the maximum reduction temperature of each peak in TPR results of each sample.

When increasing the alkali concentration to 2.0 M, the XRD patterns exhibited the characteristic reflections of LDH carbonates with a series of (0 0 1) peaks appearing as narrow symmetric lines, corresponding to the basal spacing and higher order reflections [16,24]. As a result, the only monophasic hydrotalcite was obtained and observed.

For the final composites obtained from the calcination of precursor, only the diffraction peaks of the CuO and ZnO phase were found, while the diffraction of Al_2O_3 phase was not detected for the entire final composite, indicating that Al_2O_3 presented as amorphous phase and was finely dispersed in the other phases. The catalysts decomposed from the precursors of CZApre-0.6 and CZApre-1.0 with the phases of copper nitrate and the malachite showed very sharp diffraction peaks of CuO and ZnO, however, the composites obtained from the pure LDHs CZApre-2.0 precursor only showed a broad peak of CuO phase but no ZnO diffraction peak. As a result, the structure and phase composition depends on the precursors formed, and the decomposition behavior of the precursors was analyzed by TG–DTG data (Fig. 2). Precursors were heated in air with a heating rate of 10 °C min^{-1}, the weak peak presented at around 100 °C was attributed to the physically adsorbed water, and the peak presented around 100–150 °C was due to the structure water [17]. Moreover, the peak presented at 240 °C should be ascribed to the decomposition of nitrate hydroxide, which was in agreement to the literature that the copper nitrate hydroxide decomposed at 160–235 °C [37]. Finally, the solid residue was CuZnAl(O) as confirmed by the XRD patterns (Fig. 1B). Furthermore, it has reported that the removed products contained HNO_3, H_2O, NO_2, O_2 from the TG-FTIR analysis. The malachite decomposed in a single step around 383 °C as seen in Fig. 2b [22,38]. A broad peak at 143 °C was attributed to the thermal decomposition of the hydrotalcite compound in Fig. 2c, resulting in the destruction of hydrotalcite framework, and the dehydroxylation and decarbonation seemed to occur simultaneously to produce the composite oxides [39]. The decomposition behavior of the precursors and the final composites

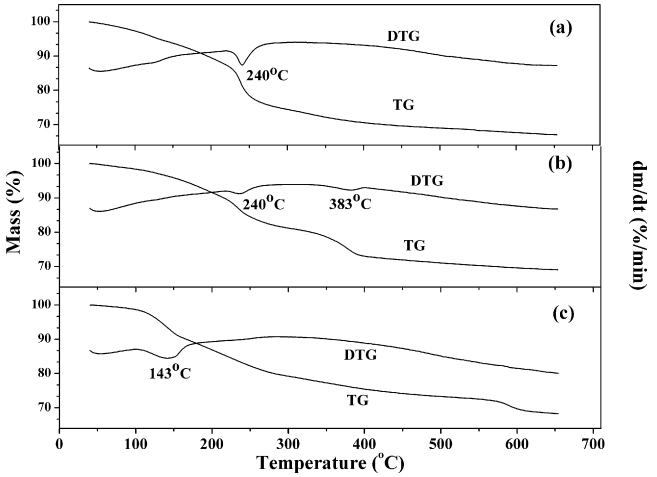

Fig. 2. TG–DTG curves of the precursors. (a) CZApre-0.6, (b) CZApre-1.0, and (c) CZApre-2.0.

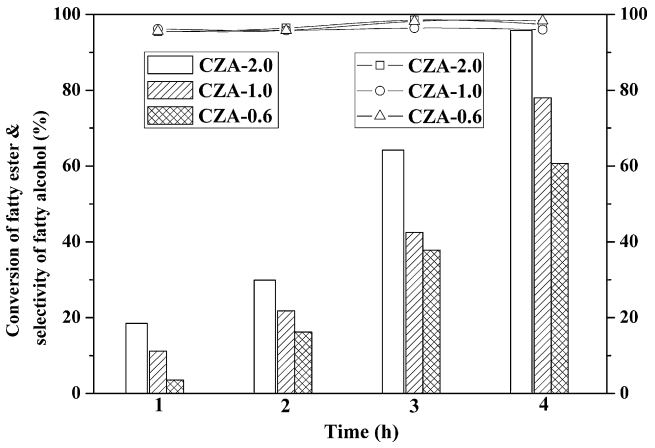

Fig. 3. A plot of the conversion (column) and selectivity (line) against the reaction time over $CuO/ZnO/Al_2O_3$ catalysts. Reaction conditions: ethyl stearate 1.0 mmol, catalyst 50 mg, hexane 5.0 ml, H_2 3.0 MPa, 230 °C.

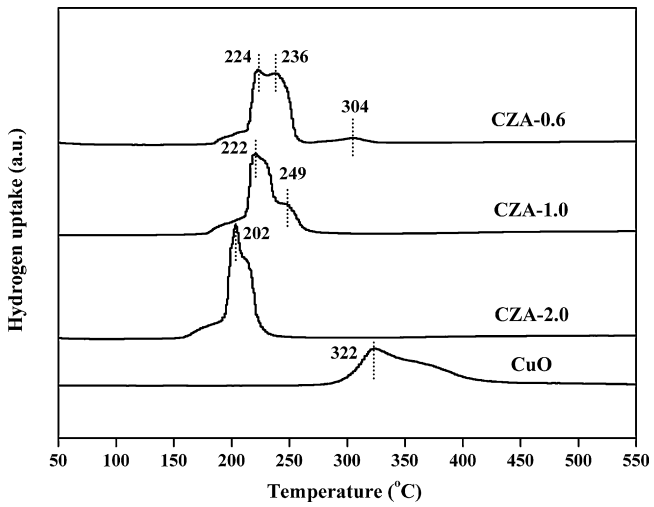

Fig. 4. TPR profiles of the catalyst prepared at different concentration of alkali.

was consistent with the observed diffraction peaks patterns and intensity of X-ray diffraction analysis.

3.2. Catalytic performance

The catalytic performance of the above composites derived from different precursors was evaluated for the hydrogenation of ethyl stearate ester, and the results are shown in Fig. 3. It was clear that the conversion of the ethyl stearate increased with the extension of the reaction time. Moreover, the conversion largely depended on the catalysts checked, for the catalysts obtained with different initial alkali concentration, the order of the conversion was CZA-0.6 < CZA-1.0 < CZA-2.0, and the conversion increased from 60% to 96% (after reaction for 4 h) when the initial alkali concentration increased from 0.6 to 2.0 M. This will be explained by their difference in the structure in detail later. It is worth noting that the stearyl alcohol was produced with a high selectivity (>97%) for all the catalysts checked. For the metal catalysts, the copper based one was more selective to fatty alcohol among the metal catalysts reported. For example, Cao and coworkers reported that both the conversion and selectivity reached above 95% for the hydrogenation of methyl laurate to lauryl alcohol over Cu/ZnO catalyst at 240 °C, in which the decrease of conversion and selectivity with increasing of the chlorine concentration was mainly discussed [23]. Liu et al. compared the $Cu–Zn/Al_2O_3$ catalyst with the commercial catalysts of Cu–Cr, Cu–Cr–Mn, and Cu–Cr–Ba, and the yield of the fatty alcohol was above 80% with $Cu–Zn/Al_2O_3$ catalyst [34]. However, the selectivity of fatty alcohol was not so satisfied over the other metal catalysts, for example, Miyake et al. [33] studied the hydrogenation of methyl laurate with Ru/Al_2O_3 and Rh/Al_2O_3 catalysts at a temperature of 300 °C, the selectivity toward lauryl alcohol was less than 20%, but it could be improved by addition of Sn to the catalysis system, however, the maximum selectivity was still less than 50%. In addition, $Ru–Sn/TiO_2$ was designed for the hydrogenation of methyl oleate to oleyl alcohol, while the activity decreased with a considerable increase of unsaturated alcohol at 250 °C, finally the yield reached about 52% after 14 h of reaction. As a result, the copper catalyst was the most used and effective catalyst for the hydrogenation of fatty acid ester to produce fatty alcohol, and it gave either high activity or high selectivity through adjusting the preparation conditions of copper catalysts. In present work, the optimized Cu/Zn/Al composite catalyst gave >98% yield of stearyl alcohol at 230 °C for 4 h reaction, which is one of the best results by comparing to literature as shown in Fig. 3.

3.3. Active species and structure effects

As the results of XRD and TGA discussed above, the composition of the formed precursor (CZApre-*x*) was largely different when the initial concentration of alkali precipitant changed, which may result in different metallic distribution of Cu, Zn and Al in the final composites (CZA-*x*), and obviously, the changes in the chemical environment of copper will affect the catalytic performance significantly [40,41]. Based on the above analysis, we speculated the obtained composites may have different kinds of copper species, and it was verified by the TPR. The reducibility of the catalysts obtained from different precursors was shown in Fig. 4. Meanwhile the maximum temperature values of each reduction peak are listed in Table 2. Obviously, the reduction temperature (peak of hydrogen exhausted), was in an order of CZA-0.6 > CZA-1.0 > CZA-2.0, suggesting the reduction peak shifted to the lower temperature. For CZA-2.0 composite, a main reduction peak presented at about 202 °C, with a smaller shoulder peak at 220 °C. By contrast, the CZA-1.0 showed reduction peaks at 222 °C and 249 °C and the CZA-0.6 at 224 °C and 236 °C, which strongly suggested the electronic environment around CuO was totally different among these three composites. For the CZA-2.0, CuO species reduced at lower temperature of 202 °C was about 85% in the total copper content, it should be the main active species. However, for the CZA-0.6, two species were equally to present at 222 °C and 236 °C and the reduction peak of the pure CuO presented at a high temperature of 322 °C, which is in agreement to those (350–450 °C) reported the literature [28,31]. Therefore, the CZA samples, especially CZA-2.0, showed a high reducibility, it was ascribed to the electronic interaction between CuO with ZnO and Al_2O_3, which altered the electronic environment of CuO and induced the CuO in CZA-2.0 to be more easily reduced at the lower temperatures. In addition, the smaller CuO particles in the CZA-2.0 sample may be another factor for the lower reduction temperature. In the XRD analysis, only one diffraction peak of CuO but no ZnO was detected in CZA-2.0, while for the composites of CZA-1.0 and CZA-0.6, both the diffraction peaks of CuO and ZnO were found. The diffraction peaks of CuO changed from sharp to flat with increasing of initial concentration of alkali in the co-precipitation (Fig. 1B), and the size of CuO particles was about 12 nm in CZA-2.0 and around 16 nm in CZA-0.6 as seen in Table 2, this may be one reason for the activity difference in the obtained three composites. Moreover, the CZA-2.0 has a LDHs structure from the XRD result of its corresponding precursor (Fig. 1Ac), a hexagonal close-packing of hydroxyl ions, with all octahedral sites every two interlayers occupied by M^{2+} ions. After partial M^{2+}/Al^{3+} substitution giving rise to

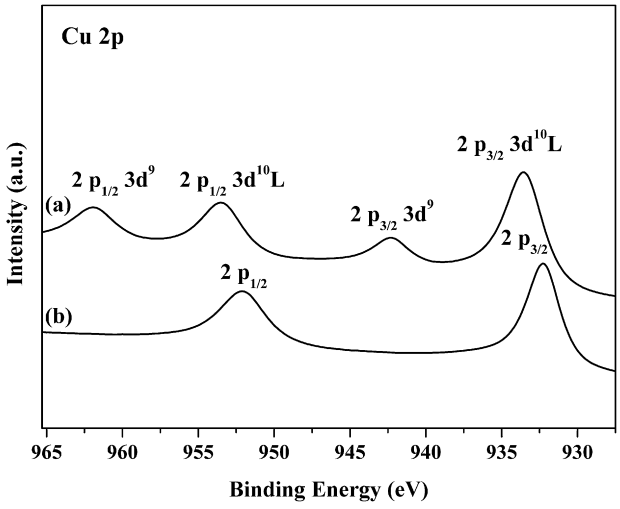

Fig. 5. XPS spectra of CZA-2.0. (a) Fresh catalyst and (b) used catalyst.

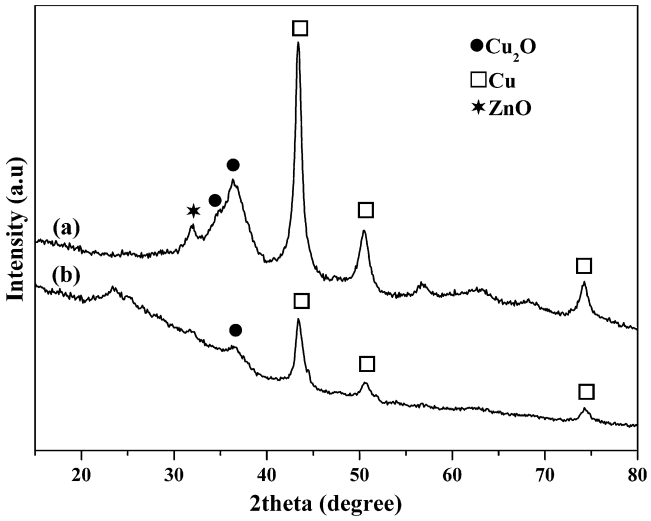

Fig. 6. The XRD patterns of CZA-2.0. (a) Used catalyst and (b) reduced catalyst.

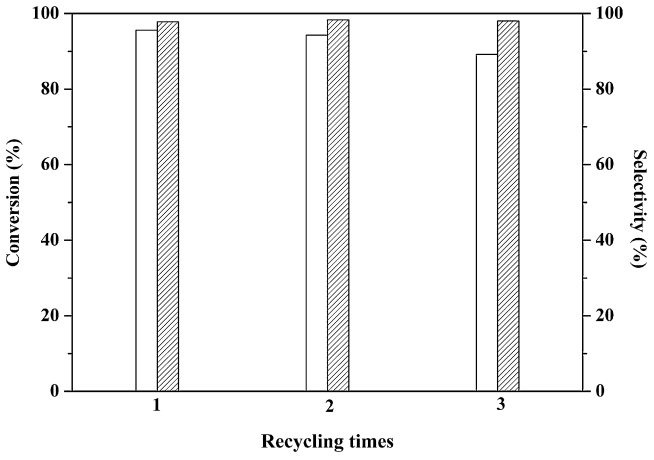

Fig. 7. Recycling results for the hydrogenation of ethyl stearate to stearyl alcohol over CZA-2.0 catalyst.

positively charged layers, thus it lead to location of anions in the interlayer space, i.e. carbonate, and water molecules [26,27]. Therefore, the highest activity of CZApre-2.0 may be ascribed to its well distribution of copper species and unique LDHs structure [4,26].

Up to now, the CuO/ZnO composite has prompted more and more fundamental work to devote to the role of each component and/or the active species [40,42–44]. The latest results reported in Science studied the active sites of Cu/ZnO catalyst from the point of the surface defects and exposure crystal facet, indicating that the ensemble of Cu steps sites and the defective ZnO_x, resulted in high activity in methanol synthesis [6]. More often, the copper active sites are studied from the point of surface chemical states. Either the reduced copper or the oxide copper is the active sites, which is still a debate issue [45,46]. Cu^+ was considered to be the active site in some cases, and the Cu^+/Cu^0 was demonstrated to be the active species in the hydrogenation with temperature programmed oxidation (TPO) with N_2O [47]. In order to explore the real active species in present reaction system, the CZA-2.0 composite was selected for comparison experiment, and the CZA-2.0 without pre-reduction treatment gave a lower conversion of 29.9%. However, that the CZA-2.0 pre-reduced at 230 °C showed a higher conversion of 71.4% at the same reaction conditions. It clearly suggested that the active site should be the lower valence copper species, and which was confirmed further by the XPS analysis.

The XPS spectra of the fresh and used samples are given in Fig. 5. The fresh catalyst displayed Cu $2p_{1/2}$ binding energies at ca. 953.5 eV and Cu $2p_{3/2}$ at 933.4 eV, as well as the satellite peaks at 941–944 eV, 959–963 eV respectively. These were characteristic of the Cu^{2+} species as described in literature [41,46]. However, for the used catalyst, the satellite peaks disappeared, and at the same time the binding energy of Cu $2p_{1/2}$ peak shifted toward 952.2 eV, and the Cu $2p_{3/2}$ shifted to 932.3 eV, indicating that the copper species transformed to the low valence copper (Cu^+ or/and Cu^0), moreover, the diffraction peak of CuO disappeared, and the new phases of crystalline Cu and Cu_2O presented in the used and the pre-reduced catalyst, thus the in situ produced Cu^+/Cu^0 species should be responsible for the high reactivity of the hydrogenation reaction, which is in agreement with the literature [42]. We certified that Cu^{2+} species could be reduced in situ to Cu^+ or/and Cu^0 under the reaction conditions (230 °C, 3.0 MPa H_2), since the reduction temperature of CuO in CZA-2.0 was lower than 220 °C, which was also certified by the results of XRD (Fig. 6), therefore, the Cu^+/Cu were the active species in our present catalytic system. In addition, the pre-reduced catalyst could be recycled for several times, although a slight loss in activity was found, which should be ascribed to the loss in the amount of catalyst during the recycling (Fig. 7). Thus, this catalyst has more potential for the industrial production of higher alcohol.

It generally was accepted that the active species of the copper catalyst was lower valence copper species in the hydrogenation reaction. Xu et al. [42] revealed that the evolution of the catalytic activity with the Cu^0 and Cu^+ surface areas, which suggested the cooperative effect was that Cu^0 dissociated hydrogen and Cu^+ activates dimethyl oxalate during the gas hydrogenation of dimethyl oxalate to ethylene glycol. It is worth to note that the active species of Cu/Zn/Al in the catalytic reactions may depend on the reaction conditions, thus the discussion of active species was still an important topic due to the versatile utilization of the Cu/Zn/Al catalysts [48].

4. Conclusions

In conclusion, the structure and activity of $CuO/ZnO/Al_2O_3$ could be controlled and optimized by varying the initial concentration of precipitant in the co-precipitation process. At the higher initial concentration of 2.0 M, the precipitated precursor has a unique structure of LDHs, and the composite derived from its calcination has smaller CuO particles about 12 nm which was highly dispersed in the amorphous ZnO

and Al_2O_3 phases. The CuO was easily reduced in situ during the hydrogenation of ethyl stearate ester at 230 °C, and the stearyl alcohol was produced with a yield > 98% under the optimum conditions. Particularly, the structure–activity relationship was discussed and the following factors have been confirmed: (1) the single LDHs phase was formed in the precipitated precursor; (2) it then thermally decomposed into smaller copper oxide and highly dispersed in amorphous zinc oxide particles; (3) stronger electronic interaction among the components of CuO, ZnO and Al_2O_3 resulted in the composite easily to be reduced in situ during the reaction; and (4) finally, the high yield (>98%) of stearyl alcohol was produced over the CZA-2.0. Moreover, the Cu^+/Cu^0 were certified to be the active species in the present hydrogenation of ethyl stearate.

Acknowledgements

The authors gratefully acknowledge the financial support from NSFC 21273222 and Jilin Provincial Science & Technology Department, China (20111802, 20100562, 20090707).

References

[1] J. Agrell, H. Birgersson, M. Boutonnet, J. Power Sources 106 (2002) 249–257.
[2] T. Takeguchi, K. Yanagisawa, T. Inui, M. Inoue, Appl. Catal. A: Gen. 192 (2000) 201–209.
[3] K.M. VandenBussche, G.F. Froment, J. Catal. 161 (1996) 1–10.
[4] Y.L. Zhang, Q. Sun, J.F. Deng, D. Wu, S.Y. Chen, Appl. Catal. A: Gen. 158 (1997) 105–120.
[5] B.A. Peppley, J.C. Amphlett, L.M. Kearns, R.F. Mann, Appl. Catal. A: Gen. 179 (1999) 21–29.
[6] M. Behrens, F. Studt, I. Kasatkin, S. Kuhl, M. Havecker, F. Abild-Pedersen, S. Zander, F. Girgsdies, P. Kurr, B.L. Kniep, M. Tovar, R.W. Fischer, J.K. Norskov, R. Schlogl, Science 336 (2012) 893–897.
[7] C.S. Chen, J.H. Lin, J.H. You, C.R. Chen, J. Am. Chem. Soc. 128 (2006) 15950–15951.
[8] S. Catillon-Mucherie, F. Ammari, J.M. Krafft, H. Lauron-Pernot, R. Touroude, C. Louis, J. Phys. Chem. C 111 (2007) 11619–11626.
[9] M. Behrens, S. Kissner, F. Girsgdies, I. Kasatkin, F. Hermerschmidt, K. Mette, H. Ruland, M. Muhler, R. Schlogl, Chem. Commun. 47 (2011) 1701–1703.
[10] M. Fu, Y.L. Li, S.W. Wu, P. Lu, J. Liu, F. Dong, Appl. Surf. Sci. 258 (2011) 1587–1591.
[11] I. Atake, K. Nishida, D. Li, T. Shishido, Y. Oumi, T. Sano, K. Takehira, J. Mol. Catal. A: Chem. 275 (2007) 130–138.
[12] J.B. Ko, D.H. Kim, Solid State Ionics Sci. Technol. Ions Motion (2004) 323–327.
[13] E.K. Poels, D.S. Brands, Appl. Catal. A: Gen. 191 (2000) 83–96.
[14] H. Praliaud, S. Mikhailenko, Z. Chajar, M. Primet, Appl. Catal. B: Environ. 16 (1998) 359–374.
[15] T. Ressler, M.M. Gunter, B. Bems, C. Buscher, T. Genger, O. Hinrichsen, M. Muhler, R. Schlogl, Catal. Lett. 71 (2001) 37–44.
[16] T. Ressler, M.M. Gunter, R.E. Jentoft, B. Bems, J. Catal. 203 (2001) 133–149.
[17] W. Fu, Z.H. Bao, W.Z. Ding, K.C. Chou, Q.A. Li, Catal. Commun. 12 (2011) 505–509.
[18] S. Fujita, A.M. Satriyo, G.C. Shen, N. Takezawa, Catal. Lett. 34 (1995) 85–92.
[19] B.L. Kniep, T. Ressler, A. Rabis, F. Girgsdies, M. Baenitz, F. Steglich, R. Schlogl, Angew. Chem. Int. Ed. 43 (2004) 112–115.
[20] T. Ressler, B.L. Kniep, I. Kasatkin, R. Schlogl, Angew. Chem. Int. Ed. 44 (2005) 4704–4707.
[21] C. Baltes, S. Vukojevic, F. Schuth, J. Catal. 258 (2008) 334–344.
[22] I. Kasatkin, P. Kurr, B. Kniep, A. Trunschke, R. Schlogl, Angew. Chem. Int. Ed. 46 (2007) 7324–7327.
[23] H. Huang, S.H. Wang, S.J. Wang, G.P. Cao, Catal. Lett. 134 (2010) 351–357.
[24] Y. Zhao, F. Li, R. Zhang, D.G. Evans, X. Duan, Chem. Mater. 14 (2002) 4286–4291.
[25] H. Zhang, Y.H. Xu, D.G. Evans, X. Duan, Acta Chim. Sin. 62 (2004) 750–756.
[26] V. Rives, M.A. Ulibarri, Coord. Chem. Rev. 181 (1999) 61–120.
[27] M. Turco, G. Bagnasco, U. Costantino, F. Marmottini, T. Montanari, G. Ramis, G. Busca, J. Catal. 228 (2004) 56–65.
[28] A. Navajas, G. Arzamendi, F. Romero-Sarria, M.A. Centeno, J.A. Odriozola, L.M. Gandia, Catal. Commun. 17 (2012) 189–193.
[29] Y. Shi, H.M. Yang, X.G. Zhao, T. Cao, J.Z. Chen, W.W. Zhu, Y.Y. Yu, Z.S. Hou, Catal. Commun. 18 (2012) 142–146.
[30] R.G. Herman, Catal. Today 55 (2000) 233–245.
[31] D.S. Brands, G. U-A-Sai, E.K. Poels, A. Bliek, J. Catal. 186 (1999) 169–180.
[32] J. Van Gerpen, Fuel Process. Technol. 86 (2005) 1097–1107.
[33] T. Miyake, T. Makino, S. Taniguchi, H. Watanuki, T. Niki, S. Shimizu, Y. Kojima, M. Sano, Appl. Catal. A: Gen. 364 (2009) 108–112.
[34] P. Yuan, Z.Y. Liu, W.Q. Zhang, H.J. Sun, S.C. Liu, Chin. J. Catal. 31 (2010) 769–775.
[35] S.G. Liang, H.Z. Liu, J.L. Liu, W.T. Wang, T. Jiang, Z.F. Zhang, B.X. Han, Pure Appl. Chem. 84 (2012) 779–788.
[36] V. Vagvolgyi, A. Locke, M. Hales, J. Kristof, R.L. Frost, E. Horvath, W.N. Martens, Thermochim. Acta 468 (2008) 81–86.
[37] X.B. Wang, L.N. Huang, T. Nonferr. Metal. Soc. 19 (2009) S480–S484.
[38] I.W.M. Brown, K.J.D. Mackenzie, G.J. Gainsford, Thermochim. Acta 75 (1984) 23–32.
[39] H. Zhang, F.Z. Zhang, L.L. Ren, D.G. Evans, X. Duan, Mater. Chem. Phys. 85 (2004) 207–214.
[40] E.I. Solomon, P.M. Jones, J.A. May, Chem. Rev. 93 (1993) 2623–2644.
[41] J. Agrell, H. Birgersson, M. Boutonnet, I. Melian-Cabrera, R.M. Navarro, J.L.G. Fierro, J. Catal. 219 (2003) 389–403.
[42] L.F. Chen, P.J. Guo, M.H. Qiao, S.R. Yan, H.X. Li, W. Shen, H.L. Xu, K.N. Fan, J. Catal. 257 (2008) 172–180.
[43] K. Teraishi, M. Ishida, J. Irisawa, M. Kume, Y. Takahashi, T. Nakano, H. Nakamura, A. Miyamoto, J. Phys. Chem. B 101 (1997) 8079–8085.
[44] Y.H. Feng, H.B. Yin, A.L. Wang, L.Q. Shen, L.B. Yu, T.S. Jiang, Chem. Eng. J. 168 (2011) 403–412.
[45] T. Genger, O. Hinrichsen, M. Muhler, Catal. Lett. 59 (1999) 137–141.
[46] G.K. Zhang, L.Q. Qin, Mater. Chem. Phys. 74 (2002) 324–327.
[47] S. Fujita, S. Matsumoto, N. Takezawa, Catal. Lett. 25 (1994) 29–36.
[48] Q. Sun, Y.L. Zhang, H.Y. Chen, J.F. Deng, D. Wu, S.Y. Chen, J. Catal. 167 (1997) 92–105.